

## ORIGINAL COMMUNICATION

---

# Technique of Semiautomatic Surface Reconstruction of the Visible Korean Human Data Using Commercial Software

JIN SEO PARK,<sup>1</sup> DONG SUN SHIN,<sup>2</sup> MIN SUK CHUNG,<sup>2\*</sup>  
SUNG BAE HWANG,<sup>3</sup> AND JINOH CHUNG<sup>4</sup>

<sup>1</sup>Department of Anatomy, Dongguk University College of Medicine, Gyeongju, Republic of Korea

<sup>2</sup>Department of Anatomy, Ajou University School of Medicine, Suwon, Republic of Korea

<sup>3</sup>Department of Physical Therapy, Kyungbuk College, Yeongju, Republic of Korea

<sup>4</sup>Department of Film, TV & Multimedia, Sungkyunkwan University, Seoul, Republic of Korea

---

This article describes the technique of semiautomatic surface reconstruction of anatomic structures using widely available commercial software. This technique would enable researchers to promptly and objectively perform surface reconstruction, creating three-dimensional anatomic images without any assistance from computer engineers. To develop the technique, we used data from the Visible Korean Human project, which produced digitalized photographic serial images of an entire cadaver. We selected 114 anatomic structures (skin [1], bones [32], knee joint structures [7], muscles [60], arteries [7], and nerves [7]) from the 976 anatomic images which were generated from the left lower limb of the cadaver. Using Adobe Photoshop, the selected anatomic structures in each serial image were outlined, creating a segmented image. The Photoshop files were then converted into Adobe Illustrator files to prepare isolated segmented images, so that the contours of the structure could be viewed independent of the surrounding anatomy. Using Alias Maya, these isolated segmented images were then stacked to construct a contour image. Gaps between the contour lines were filled with surfaces, and three-dimensional surface reconstruction could be visualized with Rhinoceros. Surface imperfections were then corrected to complete the three-dimensional images in Alias Maya. We believe that the three-dimensional anatomic images created by these methods will have widespread application in both medical education and research. Clin. Anat. 20:871–879, 2007. © 2007 Wiley-Liss, Inc.

**Key words:** semiautomatic surface reconstruction; Visible Korean Human; commercial software; three-dimensional image

---

## INTRODUCTION

In serially sectioned images of the human body, such as those generated by computed tomography or magnetic resonance, the contours of an anatomic structure can be clearly delineated. By stacking the serial images of the delineated anatomic structure and then performing surface reconstruction, a three-dimensional (3D) image can be re-created (Gehrman et al., 2006). Unlike that made by volume reconstruction, a 3D image made by surface reconstruction has very small file size, therefore, it can be dis-

Grant sponsor: Korea Science and Engineering Foundation; Grant number: R01-2005-000-10197-0.

\*Correspondence to: Dr. Min Suk Chung, Department of Anatomy, Ajou University School of Medicine, Suwon 443-749, Republic of Korea. E-mail: dissect@ajou.ac.kr

Received 4 March 2007; Revised 8 June 2007; Accepted 19 July 2007

Published online 22 October 2007 in Wiley InterScience (www.interscience.wiley.com). DOI 10.1002/ca.20535

**TABLE 1. Sequential Techniques of Semiautomatic Surface Reconstruction, Commercial Software Used, and Resultant Images**

Technique (software)	Resultant images (file format)	Number	Total file size
1. Serial sectioning of a cadaver	Anatomic images (TIFF)	976	3.6 GB
2. Drawing of selected structures (Photoshop)	Segmented images (PSD)	976	15.3 GB
3. Isolating of selected structures (Photoshop)	Isolated segmented images (AI)	15,758	15.3 MB
4. Stacking of contours (Maya)	Contour images (DXF)	114	12.6 MB
5. Filling of contour gaps with surfaces (Rhino)	Contour 3D images (DXF)	114	136.8 MB
6. Deleting of contours (Maya)	3D images (DXF)	114	47.7 MB
7. Assembling of 3D images (Maya)	Assembled 3D images (MA)	1	50.0 MB

played and rotated in real time (Shahidi, 1996). To create 3D anatomic images, automatic surface reconstruction has earlier been attempted using specifically programmed software; however, it has been exceptionally difficult to program the software to produce satisfactory images. Manual surface reconstruction has also been performed using commercial software such as Discreet™ 3ds MAX version 5.0. Nevertheless, this method has limited application because of lengthy processing times and difficulty in retaining original anatomic shapes and dimensions (Lee et al., 2005). Consequently, we considered semiautomatic surface reconstruction as an alternative for constructing 3D images of anatomic structures, using popular commercial software.

This article describes the technique of performing semiautomatic surface reconstruction of anatomic images using commercial software. This will enable anatomists and other scientists to perform surface reconstructions more quickly and objectively. This technique was developed while using serially sectioned images from the Visible Korean Human (VKH) project (Park et al., 2005b, 2006). From the 976 anatomic images of the left lower limb of the cadaver from the VKH, we chose 114 anatomic structures to study. These 114 anatomic structures were then outlined or segmented using Adobe™ Photoshop version 7.0 (Photoshop). 3D images were then constructed using Alias™ Maya version 7.0 (Maya) and Rhinoceros™ version 3.0 (Rhino).

## MATERIALS AND METHODS

### A Male Cadaver was Serially Sectioned to Create Anatomic Images

In the Visible Korean Human (VKH) project, a male cadaver was serially sectioned at 0.2 mm intervals. The sectioned surfaces were then photographed using a digital camera (resolution, 3,040 × 2,008) to create anatomic images [tag image file format (TIFF); pixel size, 0.2 mm] (Park et al., 2005b, 2006). From 8,510 anatomic images comprising the VKH data, we selected 976 anatomic images of the left lower limb, which were then cropped for further processing (file names, 1.tif, 2.tif, ..., 976.tif; intervals, 1.0 mm; resolution, 1,200 × 1,100; pixel size, 0.2 mm) (Table 1).

### Anatomic Structures were Segmented Using Photoshop

From the 976 anatomic images of the left lower limb, 114 individual anatomic structures (skin, bones, knee joint

structures, muscles, arteries, nerves) were chosen to be segmented or outlined (Table 2) using Photoshop.

We converted the file format of the anatomic images from TIFF to Photoshop Document (PSD). Then, several selected anatomic structures were outlined automatically by the Magic Wand Tool, semiautomatically by the Magnetic Lasso Tool, or manually by the Lasso Tool. Incorrect outlines were corrected either semiautomatically by the Magnetic Lasso Tool or manually by the Lasso Tool. This process was repeated for all 976 anatomic images of the left lower limb, so that 976 segmented images (file names, 1.psd, 2.psd, ..., 976.psd; intervals, 1.0 mm; resolution, 1,200 × 1,100; pixel size, 0.2 mm) were prepared (Fig. 1) (Table 1) (Park et al., 2005a).

### Patella was Selected to Prepare Isolated Segmented Images Using Photoshop

We used the following technique to create 3D images of the patella. In 45 segmented images of the patella (453.psd through 497.psd), the outline of patella was converted from a bitmap image to a vector image by using the Make Work Path Tool in Photoshop. This could be done automatically in all 45 segmented images of the patella by using the Action and Batch Tools. At this time, the tolerance, which is the distance between neighboring vector points of the images, was adjusted to 2 pixels. When tolerance was less than 2 pixels, the file size of the isolated segmented images would undesirably be increased. Conversely, when tolerance was greater than 2 pixels, shape of resulting images would be different from the original structures.

The PSD files were then converted into Adobe Illustrator (AI) files to prepare isolated segmented images of the patella, so that the contours of the structure could be viewed, independent of the surrounding anatomy. All 45 segmented images of the patella were automatically saved as AI files (453.ai through 497.ai; intervals, 1.0 mm; resolution, 1,200 × 1,100; pixel size, 0.2 mm). The AI files were designated as the isolated segmented images of the patella (Fig. 1) (Table 1).

### The Isolated Segmented Images of the Patella were Stacked to Create a Contour Image Using Maya

The isolated segmented images of the patella (453.ai through 497.ai) were opened in Maya, commercial software used to produce polygonal 3D images. Isolated segmented

**TABLE 2. One-Hundred Fourteen Segmented Structures in the Left Lower Limb, Categorized by System and Region**

System	Region	Segmented structure
Skin (1)	Skin	
Bones (32)	Pelvic bone (2)	Sacrum, hip bone
	Bones of thigh (2)	Femur, patella
	Bones of leg (2)	Tibia, fibula
	Tarsal bones (7)	Talus, calcaneus, navicular, medial cuneiform, intermediate cuneiform, lateral cuneiform, cuboid
Knee joint structures (7)	Metatarsal bones (5)	All five metatarsal bones
	Phalanges (14)	All proximal, middle, and distal phalanges
Muscles (60)	Anterior compartment of thigh (10)	Lateral meniscus, medial meniscus, anterior cruciate ligament, posterior cruciate ligament, fibular collateral ligament, tibial collateral ligament, patellar ligament
	Posterior compartment of thigh (11)	Iliopsoas, iliacus, psoas major, tensor fasciae latae, sartorius, rectus femoris, vastus lateralis, vastus intermedius, vastus medialis, articularis genu
	Medial compartment of thigh (6)	Gluteus maximus, gluteus medius, gluteus minimus, piriformis, obturator internus, superior gemellus, inferior gemellus, quadratus femoris, biceps femoris, semitendinosus, semimembranosus
	Anterior compartment of leg (4)	Pectineus, adductor longus, adductor brevis, adductor magnus, gracilis, obturator externus
	Posterior compartment of leg (7)	Tibialis anterior, extensor digitorum longus, fibularis tertius, extensor hallucis longus
	Lateral compartment of leg (2)	Gastrocnemius, soleus, plantaris, popliteus, tibialis posterior, flexor digitorum longus, flexor hallucis longus
	Dorsum of foot (2)	Fibularis longus, fibularis brevis
	1st layer of sole (3)	Extensor hallucis brevis, extensor digitorum brevis
	2nd layer of sole (5)	Abductor hallucis, abductor digiti minimi, flexor digitorum brevis
	3rd layer of sole (3)	Quadratus plantae, lumbricales (4)
Arteries (7)	4th layer of sole (7)	Flexor hallucis brevis, flexor digiti minimi brevis, adductor hallucis
		Dorsal interossei (4), plantar interossei (3)
		Internal iliac artery, external iliac artery, femoral artery, deep femoral artery, popliteal artery, anterior tibial artery, posterior tibial artery
Nerves (7)		Obturator nerve, femoral nerve, sciatic nerve, tibial nerve, common fibular nerve, superficial fibular nerve, deep fibular nerve

The values in parentheses indicate the number of segmented structures.

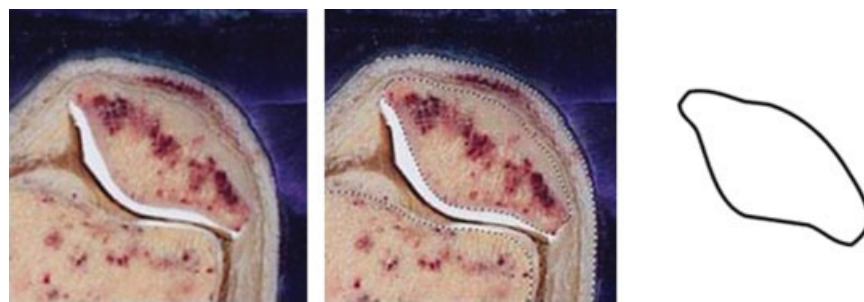


**Fig. 1.** Creating an isolated segmented image of the patella. Anatomic cross-sectional view of the left knee and patella (left). Segmented image of selected tissues, including the patella, distal femur, and overlying

ing skin (center). Resultant isolated segmented image of the patella (right). [Color figure can be viewed in the online issue, which is available at [www.interscience.wiley.com](http://www.interscience.wiley.com).]

**TABLE 3. Maya SCRIPT Used for Opening and Moving Isolated Segmented Images of the Patella to Construct a Contour Image**

```

illustratorCurves -ch 0 -ifn "c:/patella/453.ai";
  move -r 0 0 -453;
illustratorCurves -ch 0 -ifn "c:/patella/454.ai";
  move -r 0 0 -454;
...
illustratorCurves -ch 0 -ifn "c:/patella/497.ai";
  move -r 0 0 -497;

```

images of the patella (from 453.ai and 454.ai) were moved along the z axis at 453 mm and 454 mm distance, respectively. This was repeated until the isolated segmented image of the patella from 497.ai was moved 497 mm distance. Eventually, all isolated segmented images were opened and moved automatically by the Maya Script Tool in Maya (Table 3). By stacking the images in this manner, the contour image of the patella could now be visualized (Fig. 2) and saved as a drawing exchange format (DXF) file (Table 1).

The contour image of the patella accurately displayed not only its spatial location, but also its original horizontal-vertical proportions. The isolated segmented images of the patella were given file names (453.ai, 454.ai, ..., 497.ai), reflecting their distances (453 mm, 454 mm, ..., 497 mm) from the first segmented image of the left lower limb. Because the individual segmented images were moved along the z axis by these distances, the contour image of the patella reflected the original location of the patella. In addition, the isolated segmented images (resolution,  $1,200 \times 1,100$ ; pixel size, 0.2 mm) had the same pixel size as the original anatomic images. As a result, the contour image, which was composed of isolated segmented images stacked at 1 mm intervals, reflected the anatomical horizontal-vertical proportions of the patella (Fig. 2).

### A Contour 3D Image of the Patella was Generated Using Rhino

Several superoinferior lines were simultaneously drawn to connect the contour lines of the contour image by using the Loft command in Rhino. As a result, the horizontal gaps between the contour lines were filled, and a lot of quadrangular curved surfaces were visualized. This was the first and the most important step in surface reconstruction using this technique. The superoinferior lines were adjusted to be nearly at right angles to the contour lines. Moreover, the number of superoinferior lines was adjusted so as to be appropriate for the number of contours. For the patella's contour 3D image, 30 superoinferior lines were drawn. The most superior and inferior contours were then filled in using the Surface From Planar Curve command and the surface reconstruction of the patella was completed (Fig. 2).

In the contour 3D image of the patella, all quadrangular curved surfaces were then converted into triangular planar surfaces using the Polygon Mesh command. The surfaces made by the Loft and Surface From Planar Curve commands were curved and mainly quadrangular, thus called nonuniform rational B-spline (NURBS) surfaces. By using the Polygon Mesh command, the surfaces were converted into triangular planar surfaces, called polygons. This was

essential for the deletion of contours that would be performed in the next stage. Conversion to a polygon surface also minimized the file size of the contour 3D images and allowed for easier correction of the surface itself as well. Automatically, the number of contour lines was either decreased in simple regions or increased in complex regions (Fig. 2). The final contour 3D image of the patella was saved as a DXF file (Table 1).

### A Contour 3D Image of Distal Femoral Condyles was Generated Using Rhino

Some anatomic structures, such as the medial and lateral condyles of the femur, have a central region that divides the structure bilaterally. Contour gaps in these dividing regions were also filled using surface reconstruction. When the isolated segmented images of this dividing region were stacked, a superior and two inferior contours could be visualized. By using the Patch command in Rhino, we could generate curved surfaces that linked all three contours. We then deleted undesirable curved surfaces below the two inferior contours by the Trim command in Rhino (Fig. 3). The central dividing region was then attached to the regions immediately superior and inferior to it, using the Loft command. Adjacent contours were then spliced together by the Join command (Fig. 4).

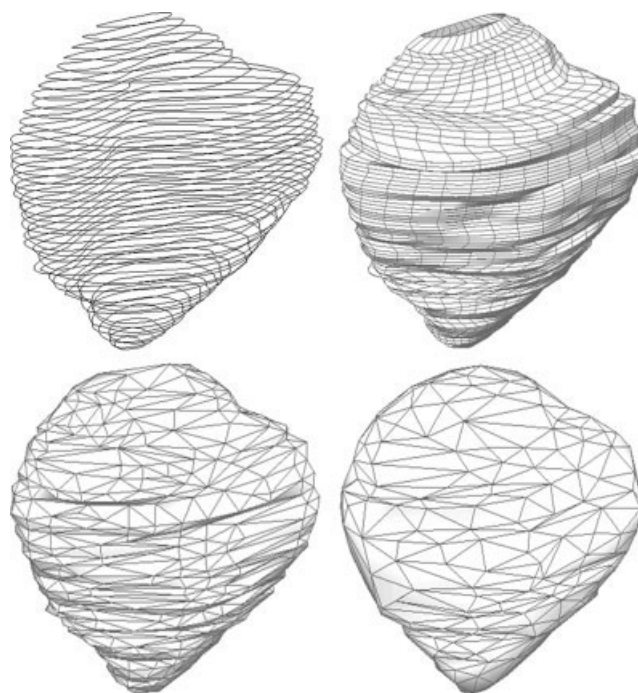


**Fig. 2.** Surface reconstruction of the patella. Contour image (top left). Contour 3D image, in which contour gaps are filled with quadrangular surfaces while the first and last contours are to be filled in (top right). Contour 3D image, in which all quadrangular curved surfaces are converted to triangular planar surfaces (bottom left). 3D image, in which contours are deleted and triangular surfaces are reduced in number (bottom right).

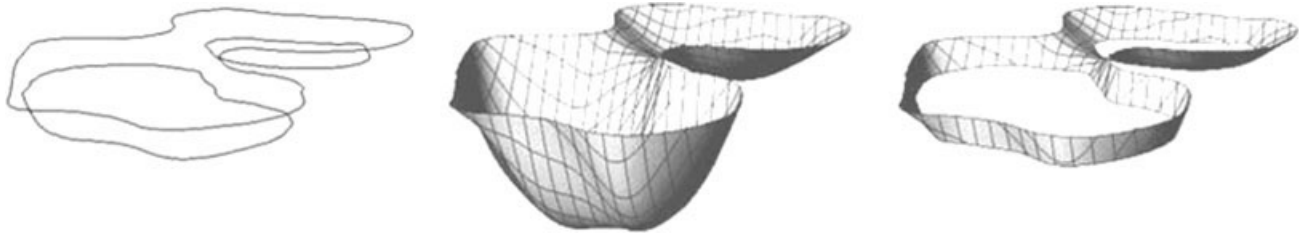


**Fig. 3.** Surface reconstruction of the central dividing region between the distal femoral condyles. Contours: one superior and two inferior (left). Curved

surfaces linking all three contours (center). Curved surfaces following deletion of undesirable curved surfaces below the two inferior contours (right).

### The Contour Lines were Deleted to Create 3D Images Using Maya

In the contour 3D image of the patella, all contour lines were deleted simultaneously by the Reduce command in Maya. The resultant image was advantageous in that it had a smaller file size, and surface errors could easily be corrected (Fig. 2). By removing specific contour lines, the total number of triangular planar surfaces of the contour 3D image could manually be reduced appropriately. Had the total number of triangular surfaces been reduced too excessively, the resultant 3D image would have been distorted from the original shape of the patella. On the other hand, had the number of triangular surfaces been reduced insufficiently, the resultant 3D image would be too difficult to correct. In the case of the 3D image of the patella, the total number of planar triangular surfaces was reduced from 2,926 to 359. The number of polygons was reduced considerably in simple regions and slightly in complex regions automatically (Fig. 5).

Distorted surface areas caused by incorrect segmentation were manually corrected until the 3D image matched the original shape of the patella. Two methods were used to accomplish this. In one method, triangular surfaces of the 3D image were moved either individually or in groups (Fig. 6). In another method, the vertices of a lattice that were dynamically linked to the triangular surfaces were moved. As a result, triangular surfaces close to the vertices were moved considerably while those far from the vertices were moved slightly (Fig. 7). After correction, several regions of the 3D image were either expanded larger than the distorted contours or shrunk smaller than the distorted contours of the patella. The result was observed by overlapping the contour image. The 3D image was then superimposed on the original anatomic structure to verify correctness of the 3D image (Fig. 8). This final form of the 3D image was saved as a DXF file as well (Table 1).

Isolated segmented images, contour images, contour 3D images, and 3D images of the other 113 structures of the lower limb were made sequentially, following the same procedure as for the patella (Table 1).

### The 3D Images were Assembled Using Maya

In a Maya ASCII (MA) file, 114 layers were created, with each layer named according to the anatomic structure it contained. For example, the 3D image of the patella (DXF

file) was opened and placed into the patella layer. 3D images of the remaining 113 structures of the lower limb were placed in their own layers and assembled until every 3D image of the lower limb could be visualized (Fig. 9) (Table 1).

## RESULTS

Since surface reconstruction was performed semiautomatically, it took only a month to construct 3D images of the 114 structures once the 976 segmented images of the anatomic structures were prepared. However, some procedures had to be manually performed. For example, to produce a contour 3D image of the patella, superoinferior lines had to be manually drawn to connect the stacked segmented images (Fig. 2). Additionally, for other anatomic structures, such as the medial and lateral condyles of the femur, there were central regions of division that had to be manually filled using surface reconstruction methods (Fig. 3). For the medial and lateral condyles of the femur, this central area of division had also to be manually attached to regions immediately superior and inferior to it as well (Fig. 4). In the contour 3D images, the total number of triangular planar surfaces was also manually reduced (Figs. 2 and 5). In these contour 3D images, flawed surface regions were also manually corrected (Figs. 6 and 7). These manual procedures required almost all of the month to complete and were performed by medical specialists with extensive knowledge of the relevant anatomy.

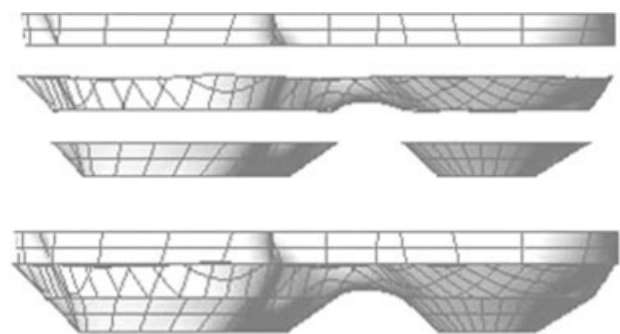


**Fig. 4.** Adjacent contours of the superior and inferior regions of the central dividing region are spliced together.

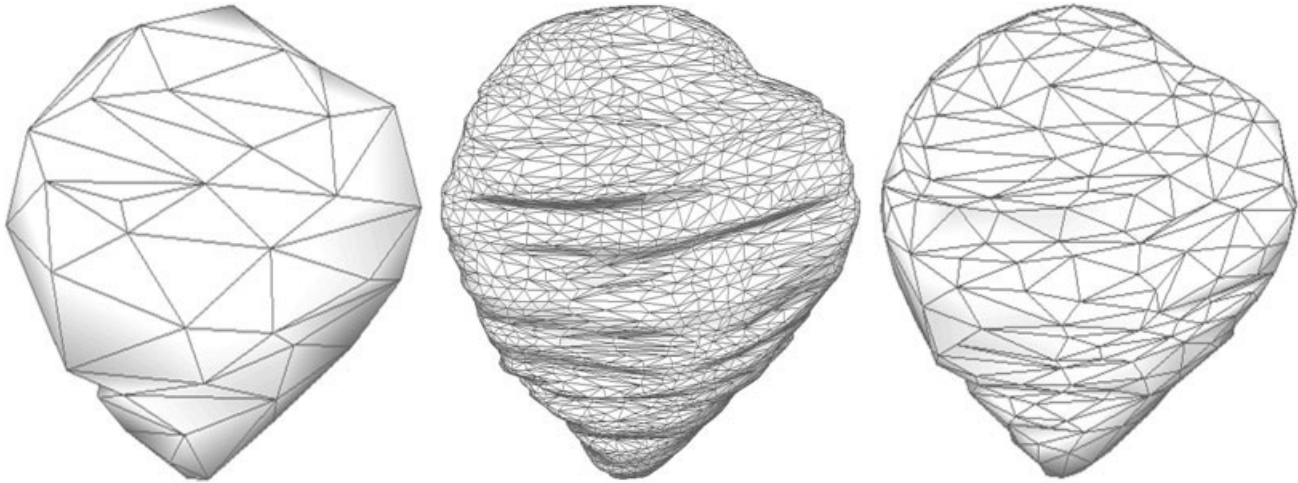


**Fig. 5.** The 3D image of the patella with 120 triangular planar surfaces (left), 2,926 surfaces (center), and 359 surfaces (right).

A composite of the 3D images generated by surface reconstruction could then be displayed in Maya. Any combination of the 3D images could be chosen and displayed in a layer window. These 3D images correctly retained the proper horizontal-vertical proportions of each anatomic structure, so that the original dimensions of the structures could readily be identified. Additionally, the 3D images reflected the proper anatomical orientation of the anatomic structures relative to its neighboring structures (Fig. 9).

The surface of each 3D image could also be colored with a specific color. After being colored with a specific color, the polygonal mesh could be made either visible or invisible. The surface color of the 3D images could also be made semitransparent (degree of transparency, 0–100%) to allow for visualization of posterior structures (Fig. 10). Furthermore, shadowing of the 3D images appeared automatically in Maya, creating a stereoscopic effect. Assembled 3D images of the lower limb could also be rotated around an axis (Fig. 11) and displayed in real

time because of the small file size of the assembled 3D images (50 MB) (Table 1).

## DISCUSSION

Finding a relatively simple and systematic way to create 3D images of anatomic structures from serial images would have widespread application in the fields of medical education and research. While the creation of 3D images by surface reconstruction can be accomplished by other means, previously attempted alternative ways seem exceedingly complicated. In the most involved method, anatomic structures can be manually drawn; however, this may require not only extreme artistic talent, but also thorough anatomic knowledge as well. Another method includes 3D scanning of anatomic structures, but internal structures such as nerves or arteries cannot be scanned. Thus, the anatomic relationship of a nerve to its neighboring structures would be impossible to study.

Therefore, we believe that semiautomatic surface reconstruction performed herein using commercial software is preferable to the above methods. It is indeed a challenging task to find or program surface reconstruction software that

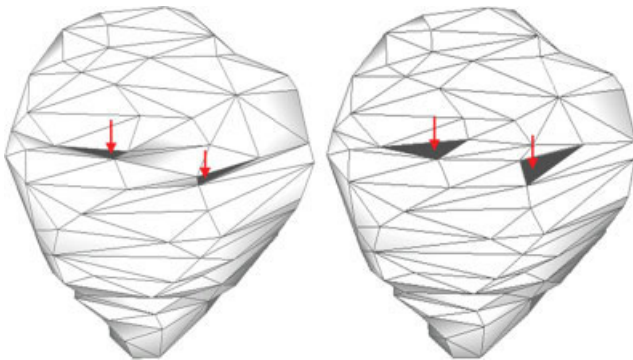


**Fig. 6.** The 3D image of the patella with incorrectly segmented regions (arrows) (left) and corrected regions (arrows) (right). [Color figure can be viewed in the online issue, which is available at [www.interscience.wiley.com](http://www.interscience.wiley.com).]

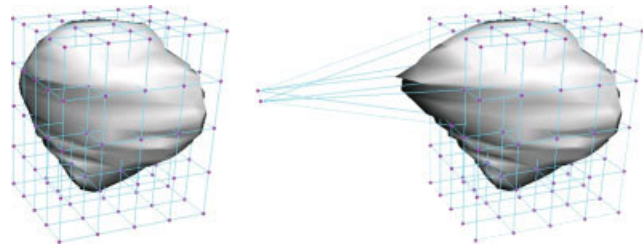


**Fig. 7.** Vertices of the lattice (left) linked dynamically to the triangular surfaces of the 3D image (right). [Color figure can be seen in the online issue, which is available at [www.interscience.wiley.com](http://www.interscience.wiley.com).]

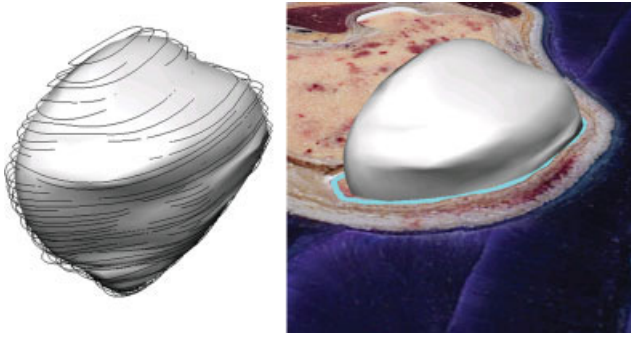


**Fig. 8.** Corrected 3D image of the patella, overlapped by the contour image (left), and superimposed on the anatomic structure (right). [Color figure can be viewed in the online issue, which is available at [www.interscience.wiley.com](http://www.interscience.wiley.com).]

would satisfy every researcher. Manual surface reconstruction using commercial software cannot be done quickly and objectively (Lee et al., 2005). Therefore, semiautomatic surface reconstruction using popular commercial software needs to be considered. Commercial software also has an advantage of being both widely available and relatively user-friendly. From our work, we recommend the following software programs for the various steps in image processing.

We used Photoshop for the preparation of isolated segmented images. The outlines of anatomic structures can be quickly and accurately drawn (Park et al., 2005a). Also, the bitmap property of the segmented images can readily be converted into the vector property (Fig. 1), which is an essential preprocess step for stacking segmented images in Maya and their eventual surface reconstruction in Rhino.

Maya was a good choice for creating contour images and contour 3D images for the following reasons. Firstly, all isolated segmented images of each anatomic structure can be opened and moved automatically (Table 3) to form contour images. Secondly, the number of triangular surfaces on the contour 3D images can be automatically decreased considerably in simple regions and slightly in complex regions opti-

mizing the small file-size of 3D images corresponding to the original shape of the structures. The contours are simultaneously deleted at the same time (Fig. 2). Thirdly, incorrect regions of the 3D image can effectively be corrected by moving triangular surfaces or the surrounding lattice. After correction, some regions of 3D images are expanded or shrunk from the original contours (Fig. 8).

We used Rhino for constructing contour 3D images. Firstly, surface reconstruction can be performed by simultaneously drawing superoinferior lines to connect the stacked contour lines (Fig. 2). Secondly, surface reconstruction of anatomic structures having central dividing regions, such as the medial and lateral condyles of the femur, can also be performed manually (Fig. 3) using Rhino. Thirdly, NURBS surfaces can be converted into polygonal surfaces using Rhino (Fig. 2), which is also advantageous: In 3D images composed of NURBS surfaces, contours cannot easily be deleted, making correction of distortions very difficult (Llic and Fua, 2006). Moreover, the file size of 3D images with NURBS surfaces, which are curved and mainly quadrangular, is 1.5 times larger than that with polygon surfaces, which are planar and triangular (Klein et al., 1996).

Selection of appropriate file formats to save the contour images, contour 3D images, and 3D images is important. We chose to save each 3D image as a DXF file since these files can be opened in popular commercial software and displayed as originally constructed. In this study, therefore, we chose DXF files not only for the 3D images, but also for interim images such as the contour images and contour 3D images (Table 1). Once the 3D images saved as DXF files are distributed, they can be widely used on many commercial softwares such as Discreet™ 3ds MAX, Autodesk™ AutoCAD, SolidWorks™ SolidWorks, and Pixologic™ ZBrush. We saved composites of the 3D images as MA files (Table 1), because they could not be saved as DXF files. Maya is a highly popular and convenient commercial software, therefore, 3D images in the MA file can easily be selected, colored, and rotated by other users (Figs. 10 and 11). It can also be verified whether the 3D images correspond to the original shape and location of the anatomic structures, while observing the 3D images on Maya. If not, the 3D images can be corrected again.

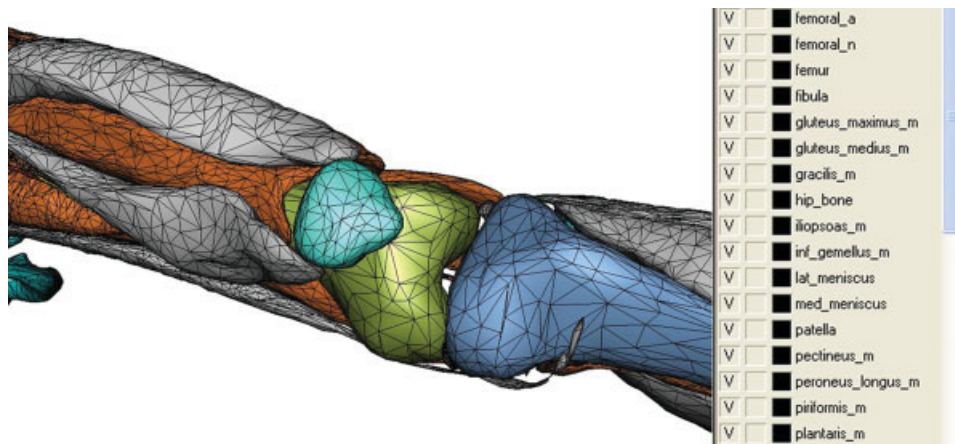


**Fig. 9.** Assembled 3D images of the lower limb, accompanied by a layer window. [Color figure can be viewed in the online issue, which is available at [www.interscience.wiley.com](http://www.interscience.wiley.com).]

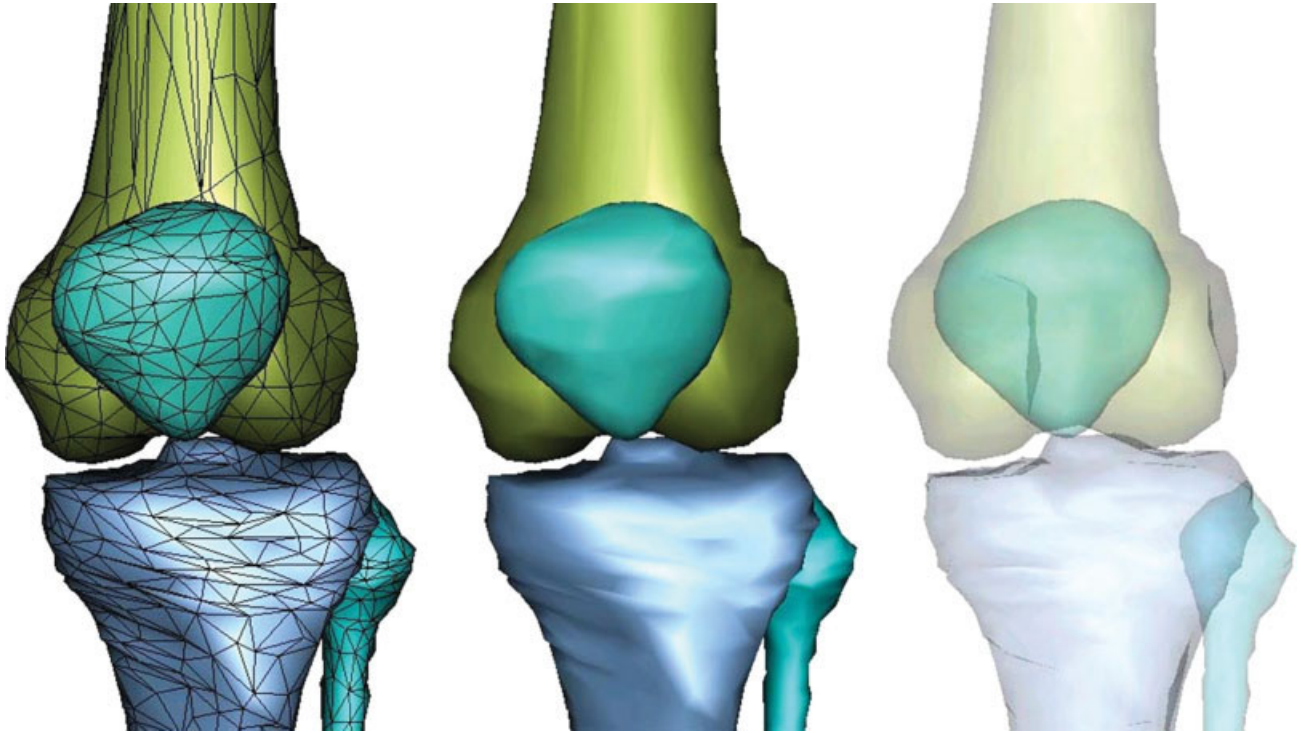


**Fig. 10.** Assembled 3D images of the bones of the knee, seen opaque with triangular surfaces (left), opaque without triangular surfaces (center), and semitransparent without triangular surfaces (right). [Color figure can be viewed in the online issue, which is available at [www.interscience.wiley.com](http://www.interscience.wiley.com).]

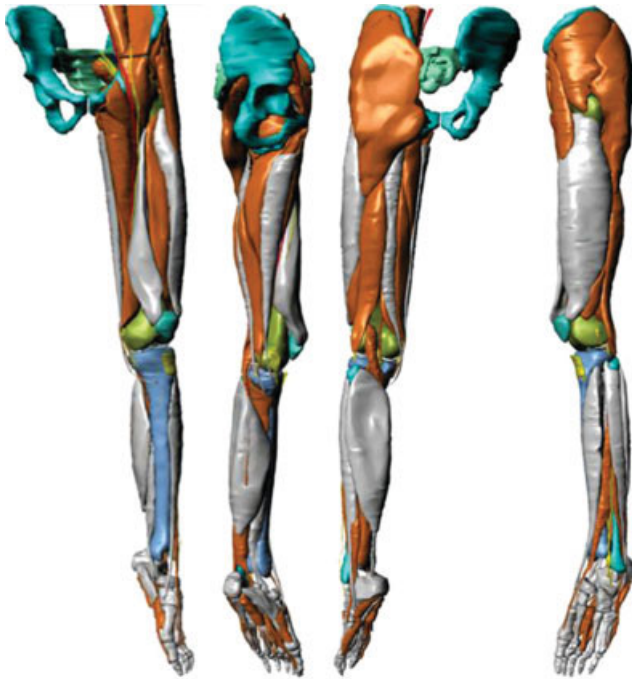


**Fig. 11.** Display of rotated 3D image of partial structures in the left lower limb. [Color figure can be viewed in the online issue, which is available at [www.interscience.wiley.com](http://www.interscience.wiley.com).]

The technique developed in this study is expected to enable researchers to conveniently perform surface reconstruction, creating 3D images from any serially sectioned images such as computed tomographs and magnetic resonance images. The commands of Photoshop, Rhino, and Maya used in this technique are also user-friendly and easily mastered.

The 3D images and assembled 3D images created in this study are also expected to be used commonly by other researchers. The images can easily be modified for further study and educational use. For example, lower limb movement such as walking can be simulated by utilizing the assembled 3D images. Accompanied by the anatomic images as well as segmented images, the 3D images generated by surface reconstruction and those by volume reconstruction can be effective tools in medical education and research (Vernon and Peckham, 2002; Pommert et al., 2006).

## REFERENCES

- Gehrman S, Höhne KH, Linhart W, Pflesser B, Pommert A, Riemer M, Tiede U, Windolf J, Schumacher U, Rueger JM. 2006. A novel interactive anatomic atlas of the hand. *Clin Anat* 19:258–266.
- Klein R, Liebich G, Strasser W. 1996. Mesh reduction with error control. *Proceeding of 7th IEEE Visualization*. p 311–318.
- Lee YS, Chung MS, Park JS, Hwang SB, Cho JH. 2005. Three dimensional MRI and software for studying normal structures of whole body. *J Korean Soc Magn Reson Med* 9:117–133.

- Lic S, Fua O. 2006. Implicit meshes for surface reconstruction. *IEEE Trans Pattern Anal Mach Intell* 28:328–333.
- Park JS, Chung MS, Hwang SB, Lee YS, Har DH. 2005a. Technical report on semiautomatic segmentation using the Adobe Photoshop. *J Digit Imaging* 18:333–343.
- Park JS, Chung MS, Hwang SB, Lee YS, Har DH, Park HS. 2005b. Visible Korean Human: Improved serially sectioned images of the entire body. *IEEE Trans Med Imaging* 24:352–360.
- Park JS, Chung MS, Hwang SB, Shin BS, Park HS. 2006. Visible Korean Human: Its techniques and applications. *Clin Anat* 19: 216–224.
- Pommert A, Höhne KH, Burmester E, Gehrmann S, Leuwer R, Petersik A, Pflesser B, Tiede U. 2006. Computer-based anatomy: A prerequisite for computer-assisted radiology and surgery. *Acad Radiol* 13:104–112.
- Shahidi R. 1996. Surface rendering versus volume rendering in medical imaging: techniques and applications. *Proceeding of 7th IEEE Visualization*. p 439–440.
- Vernon T, Peckham D. 2002. The benefits of 3D modelling and animation in medical teaching. *J Audiov Media Med* 25:142–148.